TECHNICAL MEMORANDUMS

NATIONAL ADVISORY COMMITTEE FOR AERONAUTICS

No. 913

MEASUREMENT OF THE TRUE DYNAMIC AND STATIC PRESSURES IN FLIGHT

By Georg Kiel

Luftfahrtforschung
Vol. 15, No. 12, December 10, 1938
Verlag von R. Oldenbourg, München und Berlin

Washington
October 1939

NATIONAL ADVISORY COMMITTEE FOR AERONAUTICS

TECHNICAL MEMORANDUM NO. 913

MEASUREMENT OF THE TRUE DYNAMIC AND STATIC PRESSURES IN FLIGHT*

By Georg Kiel

The apparatus for measuring the dynamic pressure in flight is almost without exception located in the disturbed velocity region of the wing. A considerable number of errors thus arise in the indications of the dynamic-pressure head and in the altimeter connected to the static-pressure head of the instrument. In the case of the biplane, there exists a region between the upper and lower wings in which the velocity is that of the undisturbed stream. In the case of the monoplane, however, within the region where the instrument may be practically installed, no position can be found at which the velocity is undisturbed and independent of the flight condition. In this report, two reliable methods are presented, with the aid of which the undisturbed flight dynamic pressure and the true static pressure may be determined without error. The second method, developed by the author, is readily applicable and in any case represents a satisfactory solution.**

INTRODUCTION

As a result of the disturbance flow about the wing, the speed instruments mounted on the airplane in general indicate a value that deviates from the true dynamic pressure corresponding to the flight velocity. The error in the indication depends on the point of installation and on the flight condition. It is of interest to know the actual

---

*"Beitrag zur wirklichkeitsgetreuen Messung des Flugstaudrucks und statischen Drucks." Luftfahrtforschung, vol. 15, no. 12, Dec. 10, 1938, pp. 583-97.

**The flight measurements were carried out by the author at the Deutsche Versuchsanstalt für Luftfahrt, Berlin-Adlershof, Institut für Flugmechanik, and the author herewith acknowledges the assistance of the DVL.

flight dynamic pressure not only in measurements of a scientific character but in practical flight operation, particularly for air transport.

It is possible of course, by calibration flights at a definite wing loading, to obtain the correct board instrument reading by a corresponding change in the scale, but in that case the correct reading will be obtained for only this one loading condition of the airplane. Since the local effect depends on the circulation, that is, on the lift coefficient, the effect changes with change in flight attitude. As soon as the wing loading deviates from that corresponding to the calibration, the readings will again be in error due to the changed lift coefficient although the dynamic pressure remains the same. It is particularly under modern flight conditions where large distances must be covered above the clouds or in blind flight that a knowledge of the true flight dynamic pressure, that is, actual flight velocity, is of considerable importance.

It is for the above reason that for some years past many airplane manufacturing firms and particularly the German Lufthansa have felt the desirability of practical investigations on the most favorable method of measuring the dynamic pressure in flight. In countries outside Germany it was also recognized that the present methods of determination of the flight velocity are still very imperfect. Thus M. Gould Beard at a session of the American Society of Automotive Engineers in Los Angeles, October 1936, in a paper on problems in the testing of transport airplanes (reference 1) also discussed velocity measurement. He expressly emphasized that the development of transport airplanes has considerably raised the accuracy requirements of the navigating apparatus and the increase in airplane size has made the pilot to a greater extent dependent on the velocity measuring apparatus. In his paper he laid particular emphasis on the fact that in the future comprehensive and practical tests will have to be conducted toward the solution of this problem on account of the importance of blind take-off and blind landing. The methods presented below for the accurate measurement of the flight dynamic pressure are designed to meet this practical requirement.

In the course of my investigations I have found that all attempts at the solution of this problem by theoretical computations failed. It is not possible with the

present airfoil theory to predict the field of flow in the immediate neighborhood of the wing with the accuracy required for practical flight operation and with a reasonable amount of computation. It is therefore attempted in this paper to solve the problem chiefly through practical flight tests.

Notation

v, velocity of flow in neighborhood of wing, (m/s).

v_∞, true flight velocity, velocity of undisturbed flow, (m/s).

q, dynamic pressure in neighborhood of wing, (kg/m^2).

q_∞, dynamic pressure corresponding to undisturbed velocity, (kg/m^2).

$\left(\frac{q}{q_\infty}\right)_o$, $\frac{q}{q_\infty}$ at $c_a = 0$.

ϵ, setting of "compensating wing" with respect to wing chord, positive with increasing angle of attack, (deg.). (See fig. 8.)

p_g, total pressure, (kg/m^2).

p, static pressure, (kg/m^2).

Subscript o denotes upper side of wing.

Subscript u denotes lower side of wing.

Subscript x denotes location of connecting tube at distance x from inlet section.

$\Delta p = p_u - p_o$, static pressure difference between upper and lower sides of wing, (kg/m^2).

l, length of connecting tube measured from entrance (narrowing in section) to exit, (m).

r, inner radius of connecting tube, (m).

u, mean velocity in the connecting tube, (m/s).

μ, viscosity, (kg/m^2).

ρ, air density, (kg^2/m^4).

$\nu = \frac{\mu}{\rho}$, kinematic viscosity, (m^2/s).

$R = \frac{ur}{\nu}$, Reynolds Number.

THE FIELD OF FLOW ABOUT THE WING

In order to bring out the difficulties to which the measurement of the dynamic pressure corresponding to the undisturbed velocity in flight is subjected, the field of flow about the wing will be briefly considered. Figure 1 shows the velocity distribution in the neighborhood of a Joukowski profile according to the computations of F. Weinig (reference 2). The curves show the lines of equal speed of flow. Figure 2 shows as a further example the results of English wind tunnel measurements (reference 4). It is of interest first to consider those positions at which the undisturbed flight speed v_∞ occurs. In figure 3 these curves, corresponding to various lift coefficients, are collected in a single diagram.* At $c_a = 0$ there are four curves along which the true flight speed is maintained ($v/v_\infty = 1$). Comparing the flow patterns for the different values of c_a, it is seen that there is a sharp change with the lift coefficient in all lines with constant v/v_∞. At large lift coefficients, of the four lines of undisturbed flow speed only two remain. As a single exception, there is a relatively small change in the curve of $v/v_\infty = 1$, starting in the neighborhood of the wing trailing edge. Also its origin remains almost unchanged. Various investigators propose instrument locations that are approximately in the neighborhood of these lines. These positions are indicated in figure 3. According to A. Lapresle (reference 6) the most favorable location lies at a distance of 25 percent of the wing chord behind the trailing edge and 35 percent above it. K. Hilding Beij (reference 8) reports on flight tests of the Pioneer Instrument Company, who used profile Gö 387 for which the pressure nozzle was located at 0.2 of the wing chord behind and 0.4 of the wing chord above the trailing edge. The value 2.4 km/h is given as the largest error. More recently, Von

*See also the work by Wieselsberger under reference 5.

Baumhauer (reference 11) has conducted similar flight tests and also wind-tunnel tests. He found the most favorable location to be 8.3 percent of the wing chord ahead of the wing triling edge and 8.3 percent of the wing chord above the upper side of the wing.

The ratio $\frac{v}{v_\infty}$ or $\frac{q}{q_\infty}$ at any position of the disturbed flow about the airfoil is not only a function of the position, but also depends on the angle of attack or the strength of circulation, i.e., on the flight attitude. In the case of the monoplane it is not possible to obtain, from a pitot-static head instrument located at a definite position on the wing, the true dynamic pressure reading or even a constant multiple of it over the entire flight range.

For the case of the biplane, the conditions are more favorable (references 13 and 14). Figure 4 shows the velocity distribution for a biplane according to computations of P. Ruden. The circulation about the upper wing induces a decrease in velocity between the surfaces of the biplane while the circulation about the lower wing induces an increase in velocity. Considering now the flow pattern between the two biplane wings, positions are found at which the decreased velocity due to the upper wing is equal to the increased velocity due to the lower wing. At these positions the resultant velocity thus corresponds to the undisturbed flow velocity. It will be further shown by flight measurements that these positions of undisturbed flow velocity are in the normal flight range practically unaffected by the flight attitude.

FLIGHT-TEST RESULTS ON THE DYNAMIC PRESSURE DISTRIBUTION FOR THE MONOPLANE

Theoretical computations on the velocity distribution in the neighborhood of an airfoil always involve some degree of uncertainty arising from the assumptions made for the computation. Wind-tunnel measurements give better results. But here, too, there are several factors involved as a result of which the velocity, or dynamic pressure distribution, in actual flight deviates from that measured in the wind tunnel. There is for one thing the effect of the different Reynolds numbers, but in many cases, too,

in wind-tunnel measurements, there is a jet overloading that affects the velocity field about the wing. In accurate measurement of the velocity distribution, the jet boundary may play a non-negligible part.

In order to learn the actual relations involved, dynamic-pressure-distribution measurements were therefore conducted on a monoplane (Junkers W 34) in flight. The dynamic-pressure distribution was determined in the neighborhood of the wing section as little affected as possible by the ailerons and propeller slipstream. There was also measured the dynamic-pressure distribution outboard of the wing tips. We shall, however, dispense with a presentation of the tests results here.

The above dynamic pressure distribution measurements in flight like the flow patterns computed by F. Weinig (reference 2) and by the results of the English wind-tunnel measurements (reference 4) show that the flow is everywhere strongly disturbed up to considerable distances from the wing. There is no position in the neighborhood of the wing of a monoplane at which, independent of the lift range, even approximately undisturbed dynamic pressure q_∞ occurs. The measurements conducted outboard of the wing tips show indeed only slight deviations from the actual dynamic pressure. The mounting of the pitot-static tubes outboard of the wing tips is inconvenient, however, in practical operation and on account of the increase in drag of the necessary outriggers is also impractical. It is frequently stated that the relations are most favorable ahead of the wing leading edge (reference 12). The arrangement of the apparatus far ahead of the wing leading edge always requires, however, inconvenient weight- and drag-increasing structures that should as far as possible be avoided. The assumption that a rod extending from the wing in the profile-chord direction leads to no appreciable increase in drag is in error since the direction of the wing is not along the rod axis. Due to the wing angle of attack and on account of the circulation about the wing, such an outrigger is attacked at an angle by the wind and results in a non-negligible increase in the drag and in addition unfavorably affects the flow about the wing on account of the vortex region generated behind the rod.

The arrangement of the apparatus proposed by many investigators in the neighborhood of the wing trailing edge (fig. 3) likewise gives no satisfactory solution. As an advantage of this arrangement, it is sometimes stated that

the pressure readings fail at the instant at which separation phenomena appear over the wing trailing edge and the pilot is thereby warned in advance of exceeding the maximum lift. On the other hand, it is known that the start of vortex shedding of the kind that disturb the instrument reading may lie within a large range of lift below the maximum. Since, furthermore, almost all modern airplanes are provided with landing flaps and similar take-off and landing aids, this proposed pitot-static tube arrangement should in many cases encounter insuperable difficulties. There is furthermore to be taken into account the fact that the altimeter in present-day practice is normally connected to the static-pressure tube of the apparatus. In a bad-weather landing the pilot would obtain an altimeter reading considerably in error even at the slightest though not dangerous stalling. According to the results thus far obtained no practical undisturbed location for the pitot-static tube can as yet be specified for the monoplane. In a later section below it will be shown what methods are available for measuring the true static pressure and dynamic pressure of undisturbed flight.

FLIGHT MEASUREMENTS FOR THE DETERMINATION OF THE MOST FAVORABLE LOCATION OF THE PITOT-STATIC INSTRUMENT IN THE CASE OF THE BIPLANE

In the case of the monoplane, we came to the conclusion that no position can be found in the immediate neighborhood of the wing at which the undisturbed-flight dynamic pressure occurs over the entire flight range. In the case of the biplane, the flow pattern shown in figure 4 indicated a large region of undisturbed flow velocity in which the instrument may conveniently be located. To check the practical utility of such an arrangement of the instrument, the flow pattern ahead of the forward strut of the N bracing of a Focke-Wulf "Stieglitz" was surveyed and the position determined at which the flight dynamic pressure occurred over the entire flight range.

To determine the undisturbed flight dynamic pressure, the readings of a Prandtl tube attached to the airplane were calibrated. In the calibration, the total pressure in the neighborhood of the wing was determined by an

apparatus developed by the author and the static pressure by means of a tube towed in the undisturbed flow under the airplane (references 15, 16, and 17). At the forward strut of the left N bracing a displaceable Prandtl tube was mounted as shown in figure 5 and the dynamic pressure measured at various points along the strut. An optical DVL double recorder was used for the dynamic pressure measurements (reference 18).

On the left of figure 5 is shown the flow effect between the biplane wings along the strut for various lift coefficients of the airplane. In order to obtain the curves of figure 5, the dynamic pressure at each measuring point was first plotted against the undisturbed-flight dynamic pressure and from the values of q and q_∞, read off from the various dynamic pressures and lifts, the ratio q/q_∞ was formed. Figure 5 clearly shows the common point of intersection of the q/q_∞ curves corresponding to the various lift coefficients. This common point of intersection lies at 0.47 wing chord above the lower wing. Furthermore, for this common point $q/q_\infty = 1$ for all curves, which shows that at this point the undisturbed flight dynamic pressure q_∞ occurs over the entire normal angle-of-attack range. A pitot head located at this position must therefore indicate the true dynamic pressure over the entire normal-flight range. Figure 6 shows a control calibration carried out with this arrangement and it is seen that the correct dynamic-pressure readings over the entire normal-flight range is confirmed. For the case of the biplane, it is in all cases possible to locate rapidly an undisturbed position between the two biplane wings.

MEASUREMENT OF THE TRUE DYNAMIC PRESSURE IN FLIGHT BY MEANS OF A PITOT HEAD AND COMPENSATING WING

1. Object of the Investigation

In the foregoing section, it was explained that in the case of the biplane there is a region between the upper and lower wings where the flow velocity is practically independent of the lift coefficient and in the entire flight range equal to the undisturbed velocity. It was therefore attempted with the aid of a small vane set above the main airfoil (in the following denoted "compensating wing" as proposed by Dr. E. Everling) to affect the air-

foil flow in such a manner that the undisturbed-flight dynamic pressure may be directly measured in its true value.

2. Test Set-Up and Measuring Apparatus

On the upper side of the right wing of a Junkers airplane (W 34) a small compensating wing was mounted (fig. 7). The dynamic pressure distribution between the compensating wing and main wing was measured with the aid of a pitot tube "rake." The compensating wing was supported by N bracings and was rotatable at points A and B. The length of the rear strut of the N bracing was variable. In this way, it was possible to vary the setting of the compensating wing with respect to the main wing chord.

The compensating wing had an N.A.C.A. M-12 section and was of constant 0.3 m chord and 2 m span. The edges were rounded. The distance between the measuring plane and the upper side of the main wing was 35 percent of the main wing chord at the measuring section. The distance of the measuring points from the airplane plane of symmetry was 3.12 m. The measuring plane was at a distance of 31.8 percent of the wing chord of the measuring section from the main wing leading edge, and was 40 mm from the leading edge of the compensating wing, that is, 13.34 percent of the compensatory wing chord and 1.41 percent of the main wing chord at the measuring position. For recording the dynamic pressures at each of the measuring positions, U tube recorders developed by the DVL were employed.

3. Measuring Procedure

The dynamic pressure distribution between the compensating and main wings was measured at various settings of the compensating wing with respect to the main wing chord. The line of reference for the setting corresponds to the line passing through the profile nose and trailing edge. The smallest setting was -6° and the largest was $+12^\circ$, where the positive sign is in the sense of increasing angle of attack. The dynamic pressure distribution measurements extended over the entire normal flight range for each constant angle of setting ϵ. In carrying out the measurements the setting was adjusted on the ground and the dynamic pressure variation between the compensating and main wing measured in flight for various dynamic pressures q_∞ and various lift coefficients c_a.

4. Results of the Dynamic-Pressure Distribution Measurements between Compensating and Main Wings

Figure 8 shows the variation of q/q_∞ as a function of the lift coefficient c_a at a few measuring points between the compensating and main wings and for the various settings ($\epsilon = -6^\circ, -3^\circ, +3^\circ, +6.4^\circ, +8.6^\circ, +12^\circ$). The ratio q/q_∞ varies with different intensity with c_a according to the setting of the compensating wing. At measuring point no. 2, which is at a distance of 2.9 percent wing chord from the lower side of the compensating wing, there appears at the settings $\epsilon = -6^\circ$, -3° and $+3^\circ$ so small a change in the dynamic pressure ratio q/q_∞ that the latter may with sufficient accuracy be considered as constant. The greatest deviations from the mean values lie on the average below 1 percent of q_∞. In the case of measuring point no. 1, which is at a distance of 1.75 percent of the main wing chord, there similarly appear at the settings $\epsilon = 6.4^\circ$ and $\epsilon = 8.6^\circ$ only slight changes in the total normal flight range. At $\epsilon = 6.4^\circ$, it may be assumed over the entire flight range that $q/q_\infty = 1.09$. Of greatest significance, however, is the result at measuring point no. 1 for a setting of $\epsilon = 8.6^\circ$. In this case, for the entire normal flight range, there may be set $q/q_\infty = 1.0$. The greatest error deviation within the limits of $c_a = 0.2$ to 1.0 then amounts to ± 1 percent of q_∞. This error, however, already lies within the measuring accuracy of the dynamic pressure determination itself. The flight velocity for this case would be determined within ± 0.5 percent of the actual flight velocity.

A clear picture of the dynamic pressure relations between the compensating and main wings is given by figure 9 showing the dynamic pressure distribution curves between the compensating and main wings for the same setting for various lift coefficients ($c_a = 0.2$; 0.5; and 1.0). The values of q/q_∞ corresponding to the various lift coefficients were obtained by interpolation from the plot of q/q_∞ against c_a. (See fig. 8.) Space limitation prevents the presentation here of the results of the individual measurements. At the small settings of the compensating wing ($\epsilon = -6^\circ$ and $\epsilon = -3^\circ$) the dynamic pressure ratio q/q_∞ at first becomes smaller with increasing distance from the compensating wing and then increases again, approaching asymptotically the value of the dynamic pressure that would exist in the absence of the compensating wing. At the settings $\epsilon = -6^\circ$ and -3°, the compensat-

ing wing produces negative lift. The result is an increase in the dynamic pressure on its under side between the compensating and main wings. At the larger settings of the compensating wing which lie in the range of positive lift, there occurs a decrease in dynamic pressure between the compensating and main wings. This decrease at large settings is greatest in the immediate neighborhood of the compensating wing and with increasing distance again approaches asymptotically the dynamic pressure which would exist in the absence of the compensating wing. The point of intersection of these curves gives the position at which q/q_∞ is independent of the flight condition and also the value of q/q_∞, which is constant over the entire angle-of-attack range. This value of q/q_∞ will be denoted by $(q/q_\infty)_{const.}$ with the arrangement investigated, the dynamic pressure curves at $\epsilon = 8.6^\circ$ intersect at $(q/q_\infty)_{const} = 1.03$ at a distance from the under side of the compensating wing of about 1.6 percent of the main wing chord at the measuring section.

Figure 10 shows the values $(q/q_\infty)_{const}$ and the corresponding distance from the compensating wing as a function of the compensating wing setting. With increasing value of ϵ the value of $(q/q_\infty)_{const}$ decreases and the point of intersection approaches the compensating wing. According to figure 10, the desired value $(q/q_\infty) = 1$ would be obtained at $\epsilon = 8.7^\circ$ at a distance of 1.7 percent main wing chord from the under side of the compensating wing, a result which is in good agreement with the corresponding values of figure 9.

5. Conclusions from the Dynamic Pressure Measurements between Compensating and Main Wings

The results of the dynamic pressure measurements between the compensating and main wings shows that it is possible with the aid of the compensating wing to affect the flow in the neighborhood of the main wing in such a manner that the undisturbed flight dynamic pressure may be measured with the required accuracy independent of the lift coefficient over the entire normal flight range. With the compensating wing arrangement investigated, the undisturbed flight dynamic pressure will be obtained at the point lying 1.7 percent of the main wing chord t be-

low the compensating wing and 1.414 percent chord from the compensating wing leading edge and at the setting $\epsilon = 8.7^{\circ}$. The ratio of compensating to main wing was 1:76.7. This result is true, however, only for the particular case of the test set-up here chosen and for the present cannot be generalized. The relations change with the shape and size of the compensating wing and particularly with the change in mounting position. Any practical applicability requires first of all a minimum expenditure in size and weight, as well as a smallest possible distance from the wing. In order to get by with a small compensating wing, it is necessary on the one hand that the mounting position be located at a position with respect to the main wing at which the velocity difference between the undisturbed and disturbed flow is the least possible and, on the other hand, it is to be taken care that the compensating wing arrangement at larger lift coefficients does not lie in the region of separation at which the reading would be in error. The choice of section of the compensating wing should also be of considerable importance. With a more highly cambered section greater velocity differences may be attained so that to obtain the same effect with a more highly cambered compensating wing section smaller dimensions would probably be required than for a section with smaller camber. A disadvantage of the method of measuring the undisturbed flight dynamic pressure by compensating wing and pitot head is the increase in drag that is associated with such an arrangement.

A NEW METHOD OF MEASURING THE TRUE DYNAMIC AND STATIC PRESSURE, PARTICULARLY ON THE MONOPLANE

1. Physical Basis of the Procedure

A very useful method by which also in the case of the monoplane the free-stream dynamic and static pressures in their true values may be directly determined, is obtained when the regions above and below the wing are simultaneously utilized for measuring the static pressure. For this purpose, the pressure heads, one above and the other below the wing, are connected with one another. Along this connecting tube from the pressure to the suction side of the wing, there is then a pressure drop or flow from below the wing to above it. It is assumed that the pres-

sure drop along the connecting tube is linear. Its length will be denoted by l. At the position x of the tube, the pressure, as may be seen from figure 11, is

$$p_x = p_u - \frac{x}{l}(p_u - p_o) \tag{1}$$

The total pressure p_g, according to the Bernoulli law is constant on the upper and lower sides of the wing, provided the flow is considered as purely potential, that is, wherever the flow is practically free from losses or vortices.

In the undisturbed flow the static pressure, from the Bernoulli equation is

$$p_\infty = p_g - q_\infty \tag{2a}$$

At any position at the upper side of the wing, the static pressure is

$$p_o = p_g - q_o \tag{2b}$$

and at the lower side

$$p_u = p_g - q_u \tag{2c}$$

We now denote the difference between the total pressure p_g at any position of the potential flow and the pressure p_x at the position x of the connecting tube as the dynamic pressure q_x, and write

$$q_x = p_g - p_x$$

Putting for p_x the expression (1) and taking account of equations (2b) and (2c), there is obtained

$$q_x = q_u + \frac{x}{l}(q_o - q_u) \tag{3}$$

Now it may be shown that under the assumption of linear pressure drop in the equalizing tube in all practical cases over the entire flight range, a value of the dynamic

pressure q_x can be obtained which is either equal to the free-stream dynamic pressure q_∞ or is a constant multiple of it, independent of the flight condition. The proof is given from the dependence of the values q_o or q_u on the free-stream dynamic pressure q_∞ and the lift coefficient c_a.

Since it is obviously unpromising to compute the field of flow with sufficient accuracy with the aid of the potential theory, we must rely on the experimental determination of the local dynamic pressure variation. In our further discussion below, we shall for this reason make use of the empirical approximation formulas obtained from flight measurements. The dynamic pressure at any position of the disturbed velocity field about the wing depends on the free-stream dynamic pressure q_∞ and the circulation or lift coefficient c_a of the wing.

Figure 12 shows the dynamic pressure ratio q/q_∞ obtained from measurements as a function of the lift coefficient c_a at various distances from the upper and lower sides of the wing. In the normal flight range the curves $q/q_\infty = f(c_a)$ are always straight lines. Denoting by $(q/q_\infty)_o$ the value of q/q_∞ corresponding to $c_a = 0$, the function $q = f(q_\infty, c_a)$ may be represented in the form

$$\frac{q}{q_\infty} = \left(\frac{q}{q_\infty}\right)_o + \frac{d}{d\ c_a}\left(\frac{q}{q_\infty}\right) c_a \qquad (4)$$

Employing, as before, the subscripts o and u for the upper and lower sides of the wing equation (3) after division by q_∞ becomes

$$\frac{q_x}{q_\infty} = \left(\frac{q_u}{q_\infty}\right)_o + \frac{x}{l}\left\{\left(\frac{q_o}{q_\infty}\right)_o - \left(\frac{q_u}{q_\infty}\right)_o\right\}$$

$$+ c_a\left[\frac{d}{d\ c_a}\left(\frac{q_u}{q_\infty}\right) + \frac{x}{l}\left\{\frac{d}{d\ c_a}\left(\frac{q_o}{q_\infty}\right) - \frac{d}{d\ c_a}\left(\frac{q_u}{q_\infty}\right)\right\}\right] \qquad (5)$$

If q_x/q_∞ is now to assume a constant value independent of the flight condition, the coefficient of c_a in brackets must be equal to zero. We must thus have the condition that

$$\frac{d}{d\,c_a}\left(\frac{q_u}{q_\infty}\right)+\frac{x}{l}\left\{\frac{d}{d\,c_a}\left(\frac{q_o}{q_\infty}\right)-\frac{d}{d\,c_a}\left(\frac{q_u}{q_\infty}\right)\right\}=0$$

This condition is satisfied if

$$\frac{x}{l}=1+\left(1-\frac{\frac{d}{d\,c_a}\left(\frac{q_o}{q_\infty}\right)}{\frac{d}{d\,c_a}\left(\frac{q_u}{q_\infty}\right)}\right) \tag{6}$$

that is, a constant dynamic pressure ratio q_x/q_∞ independent of the lift coefficient over the entire flight range will be obtained if the static pressure in the connecting tube is taken at a position at which the ratio x/l assumes the value given by equation (6). It is naturally assumed that $0 < x/l < 1$. The value of the ratio $q_x/q_\infty = (q/q_\infty)_{const}$ itself is obtained from the remaining part of equation (5) by substituting the value of x/l determined from equation (6). We thus have

$$\left(\frac{q}{q_\infty}\right)_{const}=\left(\frac{q_u}{q_\infty}\right)_o+\frac{x}{l}\left\{\left(\frac{q_o}{q_\infty}\right)_o-\left(\frac{q_u}{q_\infty}\right)_o\right\} \tag{7}$$

The value of $(q/q_\infty)_{const}$ and of the position x/l may also be graphically obtained in a simple manner. For this purpose, as schematically shown in figure 13, the values of q/q_∞, at the upper and lower sides of the wing, determined from flight tests for various flight conditions (various lift coefficients or free-stream dynamic pressures) are plotted on a common abscissa for various values of x/l and joined. The joining lines then in all cases intersect in a common point. By taking the static pressure at the position of the connecting tube indicated by the point of intersection of the straight lines there will be obtained a dynamic pressure ratio q/q_∞ independent of the flight condition. At the same time the constant value $(q/q_\infty)_{const}$ can be read off from the diagram. The magnitude of this value varies with the mounting location of the static pressure tubes. For thick wing sections, the value of $(q/q_\infty)_{const} > 1$ where the effect of the axial compression flow is large. In the region near the wing,

in which only the pure circulation is observable and the increase in velocity due to the compressed air mass vanishes, it will be possible to obtain the value $(q/q_\infty)_{const} = 1$. This should be the case particularly in the region of the wing leading edge.

2. Flow Relations in the Connecting Tube

a) Condition for linear pressure drop.- The above described method is based on two assumptions. It is first assumed that no error results in the static pressure readings from the fact that the air flows in at the lower side of the wing and out at the upper at the pressure orifices. This requirement may in all cases be easily satisfied. It is sufficient, in general, if the cross section areas of the pressure orifices (slots in the normal Prandtl tube) are a multiple of the cross section of the connecting tube. The mass of air then flowing per time unit through the narrow section of the connecting tube is then distributed at the inlet and outlet over the larger cross section of the static pressure orifice, so that only a slight disturbance of the flow occurs which practically has now no effect on the readings. Also, all sections ahead of the inlet to the connecting tube must similarly be larger than the cross section of the connecting tube, which is always more narrow. The second and most important assumption is that of linear pressure drop in the connecting tube.

It still remains to be investigated what conditions are to be satisfied in order that a linear pressure drop should be assured. It is convenient first to require a laminar flow in the connecting tube for the simple reason that this is the only type of flow that can be treated by simple methods. For the pressure drop for laminar flow in pipes, the Hagen-Poiseuille law applies according to which the pressure drop in the connecting tube is

$$\Delta p = p_u - p_o = 8 \mu \frac{lu}{r^2} + \rho u^2 \qquad (8)$$

where μ is the viscosity; l, the length of the tube measured from the entrance (narrowing in cross section) to outlet; r, the inner radius; ρ, the density; and u, the mean velocity in the tube.

At small velocities u the term ρu^2 of equation (8) becomes negligibly small. The pressure drop may then with sufficient accuracy be denoted as linear. If the condition is imposed that the error at the outlet cross section of the tube may amount at most to 1 percent of Δp, we have

$$100 \rho u^2 \leqq \Delta p$$

By solving the simplified equation (8) for u and substituting in this expression, there is obtained

$$100 \rho \Delta p \frac{r^4}{8^2 \mu^2 l^2} \leqq 1$$

Solving this inequality for l there is obtained

$$l \geqq 1.25 r^2 \frac{\sqrt{\rho \Delta p}}{\mu} \qquad (9a)$$

In order to obtain a linear pressure drop with sufficient accuracy, the dimensions of the connecting tube must be so chosen that the inequality (9a) is satisfied. Setting $\rho = 0.132$ (kgs^2/m^4) and $\mu = 1.712 \times 10^{-6}$ (kgs/m^2) (corresponding to $b = 760$ mm Hg and $t = 0^\circ$ C.), we have

$$l \geqq 265{,}000 r^2 \sqrt{\Delta p} \quad (m) \qquad (9b)$$

b) Critical Reynolds Number as limiting condition for laminar flow.- As already mentioned, equation (8) and the inequalities (9a) and (9b) developed from it are valid only for the laminar type of flow. It will therefore be further indicated under what conditions the flow is laminar.

Experience shows that, for given conditions starting from small velocities, laminar flow is first set up in the pipe. As the speed is slowly raised, there occurs at a certain speed more or less clearly defined, a sudden transition from the laminar to the turbulent condition. From the law of similarity, however, the velocity alone cannot be the determining factor for the transition from laminar to turbulent flow and the flow relations are more generally described when referred to the Reynolds Number. The

transition must thus occur at a quite definite, so-called "critical" Reynolds Number.

The transition from laminar to turbulent flow shows up with particular clearness on consideration of the resistance since the two types of flow have each their own resistance laws. For tubes of circular cross section, the Hagen-Poiseuille law is valid for laminar flow (equation (8)). In the transition from the laminar to the turbulent condition, there is a discontinuous increase in the resistance. These relations are very clearly brought out in the textbook by Prandtl-Tietjens.* Figure 14 shows these relations, the resistance coefficient

$$\lambda = \frac{\Delta p}{\frac{\rho u^2}{2}} \frac{r}{l}$$

being plotted as a function of the Reynolds Number $R = \frac{ur}{\nu}$.

Below $R = 1100$ to 1400, the resistance coefficients follow the Hagen-Poiseuille law of laminar flow.** There is then a sudden dicontinuous rise in the resistance coefficient up to a certain maximum after which it again decreases with increasing Reynolds Number. In the region of the discontinuous increase, the actual transition from the laminar to the turbulent flow occurs. That value of R at which the resistance begins to depart from the Hagen-Poiseuille straight line $\lambda = 16/R$ is denoted as the critical Reynolds Number and the corresponding velocity as the critical velocity.

The tests conducted by various investigators show that the critical Reynolds Number is a function of the initial disturbance, increasing with decrease in initial disturbance. As the various tests have shown there is a lower limiting value of the critical Reynolds Number which lies at about $R = 1000$. Below this value even the strongest disturbances decrease with time, which means that no turbulent flow can continuously be maintained below $R = 1000$.

---

*See Prandtl-Tietjens, Hydro- und Aeromechanik, vol. 2, p. 33, fig. 17.

**On neglecting the last term (ρu^2) in equation (8), there is obtained $\lambda \equiv \frac{\Delta p}{\frac{\rho u^2}{2}} \frac{r}{l} = \frac{16 \mu}{\rho u r} = \frac{16}{\frac{r u}{\nu}} = \frac{16}{R}$.

In order that the laminar flow may exist in all cases in the connecting tube, the Reynolds Number should not exceed the value 1000. We thus obtain as a second condition

$$R \equiv \frac{u\,r}{\nu} \leqq 1000 \tag{10}$$

Substituting the velocity u obtained from the simplified equation (8) (neglect of the term $\rho\,u^2$) in formula (10), there is obtained the condition

$$R \equiv \frac{\Delta p}{8\,\mu\,\nu}\,\frac{r^3}{l} \leqq 1000$$

Since we are interested in the values of l and r, we write this further condition in the clearer form

$$l \geqq \frac{1}{8000}\,\frac{\Delta p\,r^3}{\mu\,\nu} \tag{11a}$$

Substituting the values $\mu = 1.712 \times 10^{-6}$ (kg/m²) and $\nu = 13 \times 10^{-6}$ (m²/s), corresponding to a pressure of 760 mm Hg and a temperature of 0° C. in inequality (11a), there is obtained finally

$$l \geqq \frac{\Delta p \times r^3}{178}\,10^9 \text{ (m)} \tag{11b}$$

c) Dimensioning the connecting tube.- In order to assure the required linear pressure drop in the connecting tube, the conditions set up in inequalities (9a) and (11a) must be satisfied by the proper choice of length and inner radius. In figure 15 the minimum lengths l_{min} of the tube for various radii r are logarithmically plotted against the pressure difference Δp according to formulas (9b) and (11b). For a given radius r, the required minimum length of tube for the maximum pressure difference Δp $(q_{\infty_{min}})$ can be read off immediately. At small values of Δp, the condition of laminar flow (inequality (11a)) is always satisfied whenever the condition for linear pressure drop (inequality (9a)) is satisfied. For large values of Δp, the relations are reversed. In this case, the condition for laminar flow requires the larger lengths of tube.

The limit up to which formula (9a) or above which formula (11a) is valid is obtained by equating the right sides of (9a) and (11a). There is then obtained at the point of intersection of the limiting curves for l_{min} from (9a) and (11a) the value of Δp:

$$\Delta p = 10^8 \mu \nu r^2$$

Below this value of Δp, inequality (9a) is to be satisfied and above it inequality (11a). The required conditions may be more clearly written

For

$$\Delta p \lessgtr 10^8 \mu \nu r^2 \quad l \quad \begin{matrix} \geqq 1.25\, r^2 \dfrac{\sqrt{\rho \Delta p}}{\mu} \\ \geqq \dfrac{1}{8000} \dfrac{\Delta p\, r^3}{\mu \nu} \end{matrix} \qquad (12a)$$

or, making use of expressions (9b) and (11b)

For

$$\Delta p \lessgtr 0.00223\, r^2 \quad l \quad \begin{matrix} \geqq 265{,}000\, r^2 \sqrt{\Delta p} \\ \geqq \dfrac{\Delta p\, r^3}{178} 10^9 \end{matrix} \qquad (12b)$$

In the range of Δp values that practically arise in our case the required condition for linear pressure drop (inequality (9a)) is normally the determining condition.

3. Results of Practical Flight Investigations

a) General considerations on the applicability of the new method.- The new method presented above of measuring the dynamic pressure has been applied to various cases. The results obtained were very satisfactory and showed the practical utility of the procedure proposed. A presentation of the results obtained on various airplanes would carry us beyond the scope of this work. There will be given only as an example the results obtained in an investigation on a Junkers Ju 52 airplane. In a series-production airplane, the undisturbed dynamic pressure and the static pressure for determining the altitude are measured with the aid of a pressure head mounted on a 1.7 m

long rod ahead of the wing (fig. 16). In spite of this massive and inconvenient structure, the readings of the dynamic and static pressure are always in error. Aside from the increase in the weight and drag, the pressure apparatus in installations of this kind is easily subjected to injuries. In what follows, it will be shown by an example in what a simple manner the actual static pressure and the undisturbed dynamic pressure may directly be measured over the entire normal flight range by the new method proposed.

b) Conduct of the test and measurement procedure.- In order to exclude as far as possible the effect of the axial compression flow and obtain the dynamic and static pressures directly in their true values the pressure heads were mounted in the neighborhood of the wing leading edge. Furthermore, they were only at a small distance from the wing in order to reduce the drag.

To determine the most favorable distance of the apparatus, Prandtl tubes were mounted whose distance from the wing could be varied. The dynamic pressure variation ($q = f(q_\infty)$) for various distances from the upper and lower sides of the wings was thus determined. Since, in the final measuring installation, the total pressure was to be determined with the instrument at the under side of the wing the total pressure was in these measurements taken only with the pressure tube of the under side of the wing. In our measurements the dynamic pressure at the lower side of the wing is therefore

$$q_u = p_{gu} - p_u$$

and that on the upper side

$$q_o = p_{gu} - p_o$$

Possible errors as a result of the yawed setting of the tubes with respect to the wind direction are contained in the values of q_u and q_o. A check flight test showed that the yawing of the instruments to the wind direction with the arrangement employed was in all cases within a permissible range.* The undisturbed dynamic pressure was

*Further data on the errors in the pitot head readings due to yawed setting with respect to the wind direction is found in the work of Kumbruch under reference 19.

measured with the aid of a total-pressure tube and a static tube was towed below the airplane (references 15, 16, and 17). The tests were conducted for straight unaccelerated flight. The mean wing loading was 67.5 kg/m².

c) Analysis of the data.- For various undisturbed dynamic pressures q_∞ there was first determined the ratio q/q_∞ as a function of the distance from the wing (fig. 17), the values of q and q_∞ being interpolated from the plot of q against q_∞. From figure 17 the distances of the double-head installation from the under and upper sides of the wing at which q/q_∞ over the entire flight range has the value 1, may be very quickly determined by trial. To determine the factor $(q/q_\infty)_{const}$ and the corresponding position at which the static pressure is taken from the connecting tube, it is best to make use of the graphic method indicated above. Figure 18 shows a graphical determination by this method of the dynamic pressure ratio $(q/q_\infty)_{const} = 1$ and the corresponding position x/l.

If the points of attachment of the pressure heads are located on the wing, i.e., on the wing chord, the same dynamic pressure ratio $(q/q_\infty)_{const}$ may be obtained for various distances of the installation from the wing. In order to obtain a clear view on this relation, there were plotted in figure 19 the lines $(q/q_\infty)_{const}$ and $x/l = const$ as functions of the distance of the installation from the upper and lower sides of the wing.* From figure 19 there can thus be obtained for the example here considered the mounting position of the apparatus at which for the total flight range $q/q_\infty = 1$. There are also drawn the curves $(q/q_\infty)_{const} = 0.99$ and $(q/q_\infty)_{const} = 1.01$. At the same time the figure indicates the positions x/l at which the static pressure is taken from the connecting tube, this position being given by the point of intersection of the lines $(q/q_\infty)_{const}$ with the lines of constant

*In order to obtain the family of curves of fig. 19, the values of $(q/q_\infty)_{const}$ for constant distance of the pitot head from the under side of the wing and the corresponding values of x/l were plotted as functions of the distance from the wing upper side. By making use of the resulting family of curves the lines $(q/q_\infty)_{const}$ and $x/l = const$ were drawn in on fig. 19.

x/l. Intermediate values may be interpolated. A consideration of figure 19 shows that small deviations from the correct location of the static pressure tubes and small displacements in the static pressure orifice at the connecting tube lead only to vanishingly small errors which are insignificant for practical flight operation. This circumstance is of great advantage for the series production of dynamic-pressure installations of this kind. According to figure 19, the true dynamic and static pressures are most advantageously obtained in the following manner.

1. The static and dynamic tubes (in our case the Prandtl tube or dynamic tube with the same characteristics and coefficients in oblique flow) are to be located at the wing leading edge at a distance of 330 mm (that is, 8.6 percent of the wing chord at the mounting position) above the upper side of the wing and under the lower side of the wing, respectively. The directions of the tubes are to be so chosen that their axes of symmetry lie, as far as possible, in the flow direction. The actual installation dimensions are shown in figure 20.

2. The static pressure orifices, those of the upper side of the wing and those of the lower side, are then to be joined by a pressure equalizing tube. A pressure orifice at a distance of 0.39 of the total length of the connecting tube computed from the inlet at the under side of the wing then gives the true static pressure over the total normal flight range. Since we tacitly assume a linear pressure drop in the tube, the latter is to have such dimensions that under all flight conditions arising the inequalities (12a) or (12b) are satisfied.

d) Results.- On the basis of the results of figure 17, the double-head arrangement and the connecting tube were mounted as shown on figure 20, from which the dimensions of the connecting tube can also be taken. To avoid disturbances of the pressure readings due to the inflowing and outflowing at the slits of the static tube, the pitot head at the under side of the wing and the static tube at the upper side of the wing were so dimensioned that their internal cross sections were everywhere greater than those of the connecting tube. The latter was made of aluminum and was of 3 mm inside radius. In order to avoid initial disturbances, the inlet to the narrower connecting tube was well rounded. The total length of the tube was 6.405 m. The maximum pressure difference normally occurring between

the lower and upper sides of the wing is about 110 kg/m^2. Computation by means of formula (9a) or (12a) or a check by means of figure 15 shows that the conditions for linear pressure drop and laminar flow are satisfied. The manner of taking the true static pressure and the location of the orifice may be seen from figure 20. Great care was taken to see that there was no narrowing or widening of section of the connecting tube.

At the position of the static-pressure orifice, a brass tube was connected, the latter being provided with several small pressure orifices. By means of a hollow ring welded along this tube as shown in figure 20, the orifices are all united. This method of taking the pressure was chosen on account of the considerable error due to the imperfect removal of the sharp edges of the orifices, which edges were thus avoided by uniting several orifices in the manner described. In order to have a convenient mounting of the connecting tube, it was rolled up into a spiral of about 0.5 m diameter. Although this arrangement is not an ideal solution, it was chosen because it was most convenient for the investigation at hand. Thus, for example by suitable arrangement of the connecting tube with respect to the dynamic-pressure meter, the effect of the centrifugal forces in curved flight can be considerably eliminated. The connecting tube diameter was purposely chosen relatively large in order to eliminate stopping up or sources of error due to moisture deposit or dust particles, etc., in the tube. With a smaller inside diameter of the connecting tube, the length may be correspondingly smaller. (See fig. 15.) The final arrangement of the double-head installation at the wing is shown in figure 21.

The check calibration carried out with the arrangement given in figures 20 and 21 is shown in figure 22. The agreement between the indicated and true dynamic pressure is very satisfactory. Since the total pressure, except for small errors due to yaw, is correctly given and only the static pressure at the mounting position of the instrument is in error, the measuring arrangement gives the true dynamic and static pressures over the entire normal flight range. The altimeter connected to the static-pressure head thus shows over the entire normal flight range the true undisturbed-air pressure or altitude. Errors in the altitude readings which, particularly in blind flight at low altitude, may become very dangerous are thus avoided. This great advantage is pointed out with par-

ticular emphasis since, in practical flight, operation cases occur where the altimeter readings deviated by 50 to 100 meters from the true value.

Figure 22 also shows the effect of the landing flap deflection on the dynamic pressure readings. With full flap deflection of 41°, the readings, particularly for large dynamic pressures, are somewhat too small. For small dynamic pressures, the reading with flap deflection practically coincides with the zero setting of the flap. The dynamic pressure range in coming to a landing with the test airplane here employed lies between about 70 and 100 kg/m^2. For a true dynamic pressure of 100 kg/m^2 and with flap fully deflected the indicated dynamic pressure deviates by 2.5 percent from the true value. For a dynamic pressure of 70 kg/m^2 also at full flap deflection, the indicated dynamic pressure again agrees with the true value.

e) Advantages and further possibilities of application.- The method given above for measuring the static pressure and the undisturbed dynamic pressure has the advantages over those heretofore employed and often involving large errors, that the true values of the static pressure or altitude and the true dynamic pressure are directly given independent of the flight condition without involving inconvenient structures that increase the weight and drag. The most convenient and safest location of the instrument appears in all cases to be in the neighborhood of the wing leading edge where the ratio $(q/q_\infty)_{const} = 1$ is most easily obtainable independent of the flight attitude. For this reason in the example here given the instrument was mounted in the neighborhood of the wing leading edge. This arrangement is not essential however. It is also possible, for example, to obtain the true value of the undisturbed dynamic pressure when the pressure head of the wing upper side is mounted in the neighborhood of the wing leading edge while that of the lower side lies considerably aft. An example is shown in figure 23 where the measured dynamic pressure at the upper and lower sides of the wing, q_o and q_u, respectively, are plotted against the true dynamic pressure q_∞ and the location of the static pressure orifice at the connecting tube determined where $(q/q_\infty)_{const} = 1$ over the entire flight range. The measuring stations of the dynamic pressure are also indicated.

The new procedure described here for measuring the dynamic pressure may be applied in all cases. There are a large number of variations possible which give the constant

ratio of indicated to true dynamic pressure $(q/q_\infty)_{const} = 1$ over the entire flight range and there are no difficulties in finding such arrangements. In all cases in which the value $(q/q_\infty)_{const} = 1$ is not obtained, there always remains the great advantage that q/q_∞ is constant over the entire flight range. With the accuracy required for practical flight operation, the arrangement employed for one airplane may directly be applied to other airplanes of the same type and interchangeability of apparatus is thus greatly facilitated.

A further possibility of application where the above method shows promise is for high-speed airplanes where even the slightest drag increases must be avoided. There is here offered the possibility of taking the static pressures simply by orifices in the upper and lower sides of the wing. There will then be required in addition only a total pressure head which can be limited to the absolutely necessary size.

In the case of airplane with landing flap with the present day mounting of the pitot-static tube the reading also changes with the flap deflection so that depending on the mounting position of the instrument there is obtained either a too large or too small dynamic pressure with flap deflection. The same applies to the static pressure or altitude. With the method here described the true dynamic pressure readings will be maintained or only slightly changed even with flap deflection.

SUMMARY

No useful method has up to the present been known for measuring the true dynamic pressure and static pressure with corresponding altitude. The theoretical computations published in the literature on the subject and also my own flight tests have shown that in the case of the monoplane in the region where the pitot-static tube may practically be mounted there is no position where, for the entire flight range, the dynamic pressure is that of the undisturbed stream.

In the case of the biplane, the relations are considerably more favorable. The field of flow between the two biplane surfaces receives a decrease in velocity due to

the circulation about the upper wing and an increase in velocity due to that about the lower wing. Considering now the field of flow between the two biplane wings, a region will be found in which the resultant velocity for all normally occurring angles of attack agrees with the undisturbed stream velocity. Experience shows that in the case of the biplane an undisturbed mounting location for the pitot-static tube may in every case be quickly and easily found.

Starting from the flow relations prevailing between the biplane wings, it is shown that also for the monoplane it is possible with the aid of a small wing (compensating wing) mounted above the main wing to modify the circulatory and axial flow at the mounting location in such a manner that the undisturbed dynamic pressure may be measured directly in its true value. A disadvantage of this method is the increase in drag involved.

Finally, as a satisfactory solution for the measurement of the true dynamic and static pressures a new method was developed which in particular is applicable in all cases to the monoplane. By this method, the static pressure leads of two dynamic or static pressure heads, one of which is mounted above and the other below the wing, are connected to each other. Along the connecting tube there then occurs a pressure drop from the lower to the upper side of the wing. If by suitable dimensioning of the pressure equalizing tube (satisfying of the conditions given by the inequality (12a) care is taken to see that the pressure drop in the connecting tube is linear a position may be found at the connecting tube at which the true static pressure is obtained independent of the flight condition. The total pressure, according to the Bernoulli law, is constant on the upper and lower sides of the wing for the case of potential flow, i.e., wherever the flow is free from losses or circulation. The total pressure therefore can be taken either at the upper or at the lower side of the wing.

Practical investigations in flight have proven the usefulness of the new procedure for measuring the dynamic pressure. Even with full flap deflection of 41° no errors in the readings occurred for small dynamic pressures; for larger dynamic pressures the maximum error amounted to -2.5 percent. The new method above described has the advantage as compared with those employed heretofore, often involving large errors, that the true values of the static

pressure or altitude and the true dynamic pressure may directly be obtained without inconvenient structures that increase the weight and drag. False readings in the dynamic pressure and errors in the altimeter reading which may become dangerous particularly in low altitude blind flying are thus avoided by this method. This advantage is of inestimable value for practical flight operation since repeated cases have occurred where in addition to considerable error in the dynamic pressure indications the altimeter readings deviated by 50 to 100 meters from the true value.

The author expresses his thanks to his teacher, Prof. Dr. Ing. W. Hoff, for encouragement in this work; also to the DVL for supplying the means for conducting the work. Furthermore he would like to thank Prof. Dr. Everling and Prof. Dr. Ing. F. Weinig for their suggestions for improvement and the interest taken.

Translation by S. Reiss,
National Advisory Committee
for Aeronautics.

REFERENCES

1. Beard, M. Gould: Problems in Testing of Airplanes for Airline Service. Paper read at National Production Meeting of Society of Automotive Engineers, at Los Angeles, Oct. 15-17, 1936.

2. Weinig, F.: Geschwindigkeit und Richtung der Strönung um ein Tragflügelprofil. Luftfahrtforschung, vol. 12, no. 7, Nov. 28, 1935, pp. 222-28.

3. Weinig, F.: Die Strönungsverhältnisse in Felde dünner, schwachgewölbter Tragflügelprofile. Z.f.a.M.M., vol. 18, no. 2, April 1938, pp. 107-21.

4. Bryant, L. W. and Williams, D. H.: An Investigation of the Flow of air Around an Aerofoil of Infinite Span. R. & M No. 989, British A.R.C., 1924.

5. Wieselsberger, C.: Linien konstanter Strönungsgeschwindigkeit. Report No. 17, Aeron. Res. Inst., Tokyo, (vol. 2, no. 5) June 1926, pp. 115-25.

6. Lapresle, A.: Contribution a l'etude expérimentale du Champ Aérodynamique autour d'un profil austentateur. Bull. Ser. Techn. Aéro., No. 43, 1927.

7. Magnan, A. and Sainte-Lague, A.: Sur la distribution des vitesses aérodynamiques autour d'un avoin en vol. Publications scientifiques et techniques du Ministere de l'Air Service des recherches de l'Aéronautique, no. 12, 1932.

8. Deij, K. Hilding: Air Speed Instruments. T.R. No. 420, N.A.C.A., 1932.

9. Tate, George: Recent Developments in Pioneer Aircraft Instruments. Aviation Engineering, vol. 7, no. 4, Oct. 1932, pp. 16-17.

10. Tate, George: Improving Airspeed Accuracy by Pitot Tube Location. Aviation, vol. 32, no. 11, Nov. 1933, p. 339.

11. Von Baumhauer, A. G.: Opstelling van een snelheidsmeter bij een vliegtuigvleugel. Versl. en Verh. Rijks-Studiedienst Luchtvaart, Amsterdam, vol. 7, 1935, pp. 142-48.

12. Gates, S. B., and Cohen, J.: Note on the Standardisation of Pitot-Static Head Position on Monoplanes. R. & M. No. 1778, British A.R.C., 1937.

13. Ahlborn, F.: Orte für die Messgeräte an Flugzeugen. Z.F.M., vol. 16, no. 1, Jan. 14, 1925, pp. 2-3.

14. Freeman, R. G.: Air Flow Investigation for Location of Angle of Attack Head on a JN4H Airplane. T.N. No. 222, N.A.C.A., 1925.

15. Kiel, Georg: Flugstaudruck-Eichung mittels Gesamtdruckgerät und einer unter dem Flugzeug nachgeschleppten statischen Sonde. Luftwissen, vol. 5, no. 6, June 1938, pp. 219-23.

16. Kiel, G.: Total-Head Meter with Small Sensitivity to Yaw. T.M. No. 775, N.A.C.A., 1935.

17. Kiel, G.: Fehlerabschätzung bei Staudruck-Eichungen mittels unter dem Flugzeug geschleppter Sonden. Luftfahrtforschung, vol. 14, no. 6, June 20, 1937, pp. 310-13.

18. Drude, W.: Flugmessgeräte. Luftwissen, vol. 4, no. 12, Dec. 1937, pp. 363-66.

19. Kumbruch, H.: Messung strömender Luft mittels Staugeräten. Forschungsarbeiten VDI, no. 240, 1921.

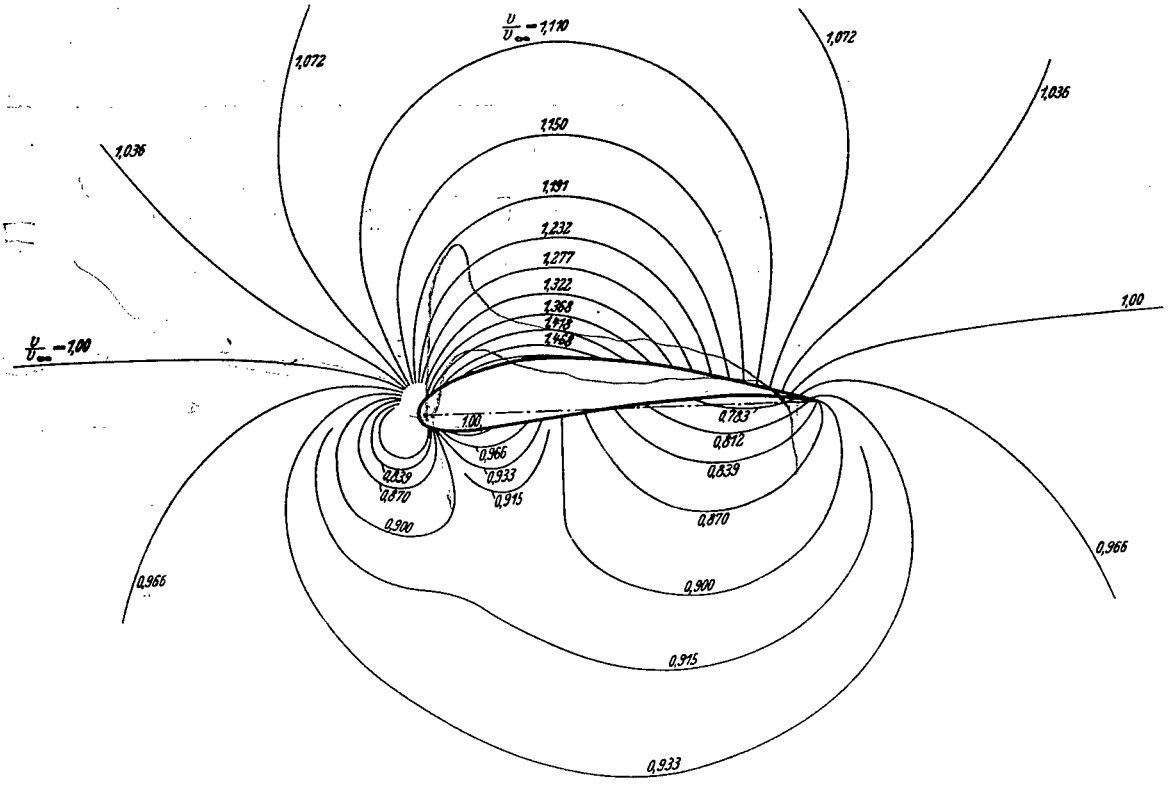

Figure 1.- Lines of equal flow speed according to computations of F. Weinig (ref. 2); angle of attack $\alpha = -50'$, lift coefficient $c_a \approx 1.1$.

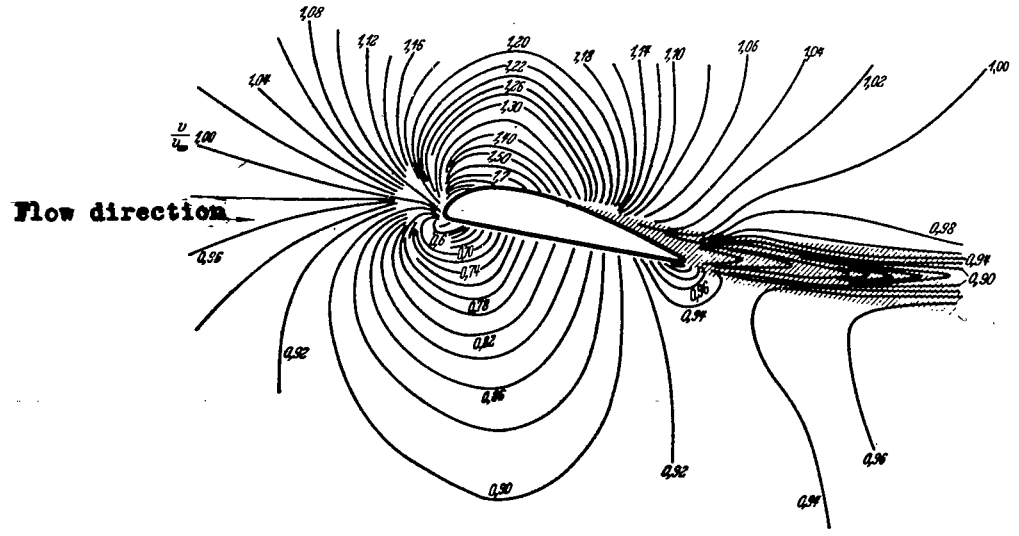

Figure 2.- Lines of equal flow speed according to computations from English wind tunnel measurements (ref. 4).

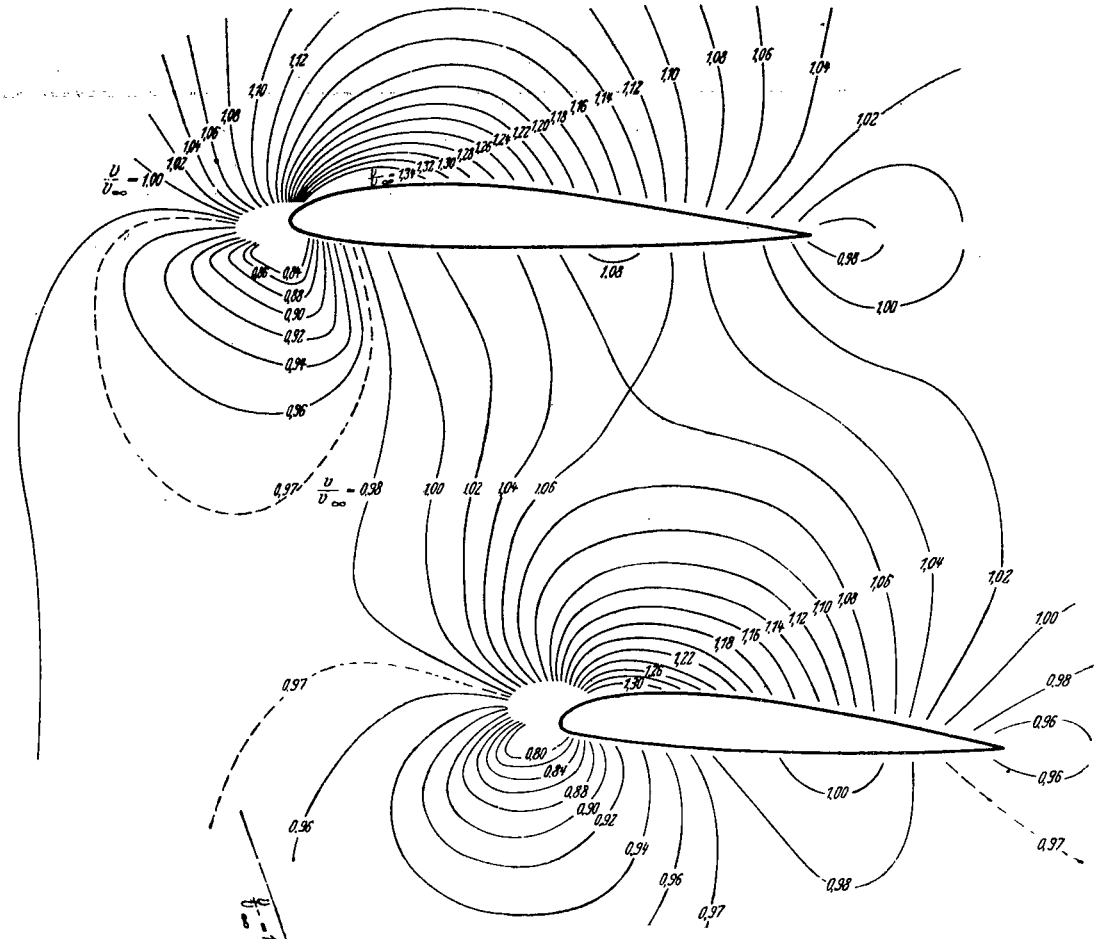

Figure 4.- Lines of equal flow speed for a biplane according to computations by P. Ruden. Normal lift coefficient of the upper wing c_{no} 0.50 " " " " " lower " c_{nu} 0.48

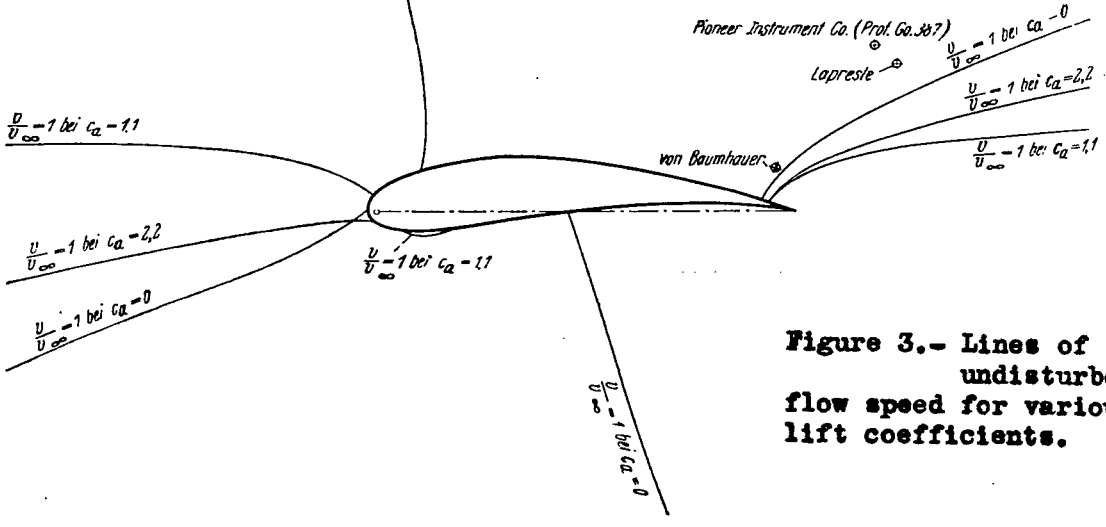

Figure 3.- Lines of undisturbed flow speed for various lift coefficients.

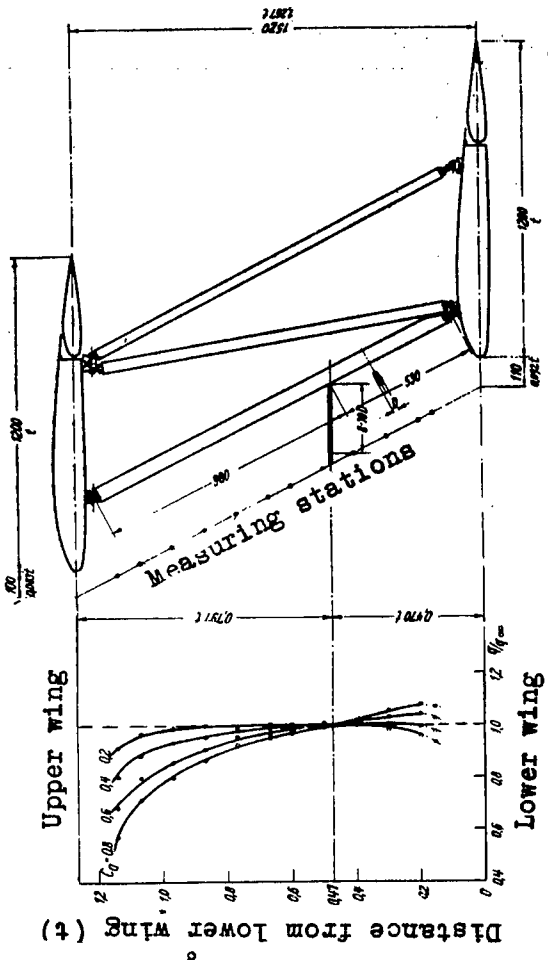

Figure 5.- Dynamic pressure ratio q/q_∞ between the biplane wings along the forward strut for various lift coefficients c_a of the airplane.

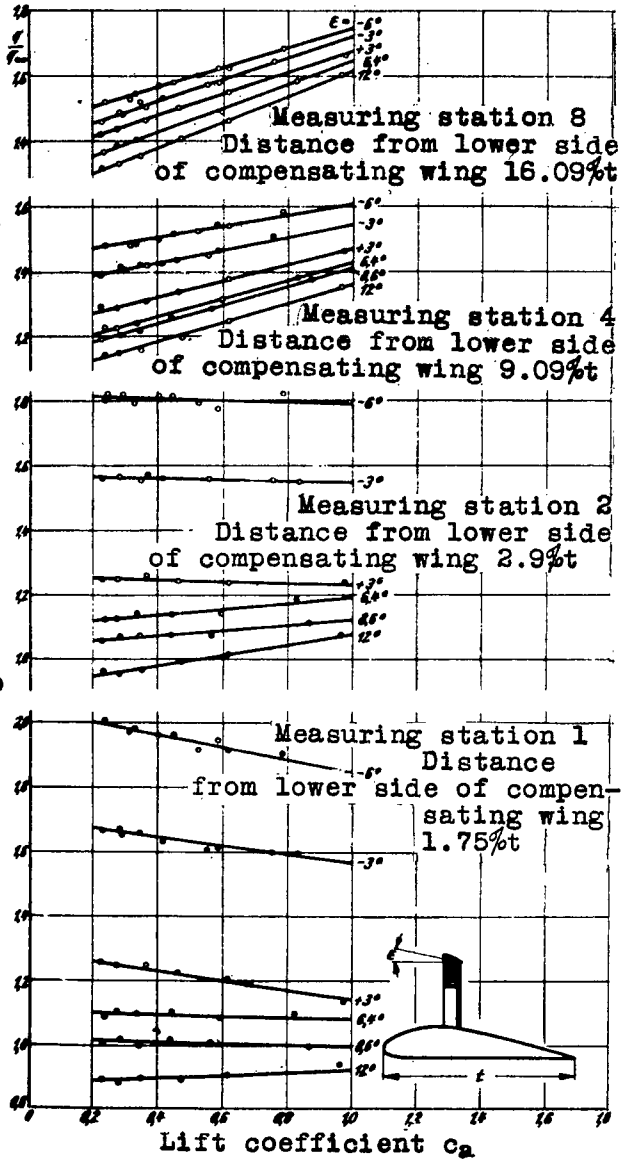

Figure 8.- q/q_∞ as a function of lift coefficient c_a at various measuring points between compensating and main wings for various settings ϵ of the compensating wing.

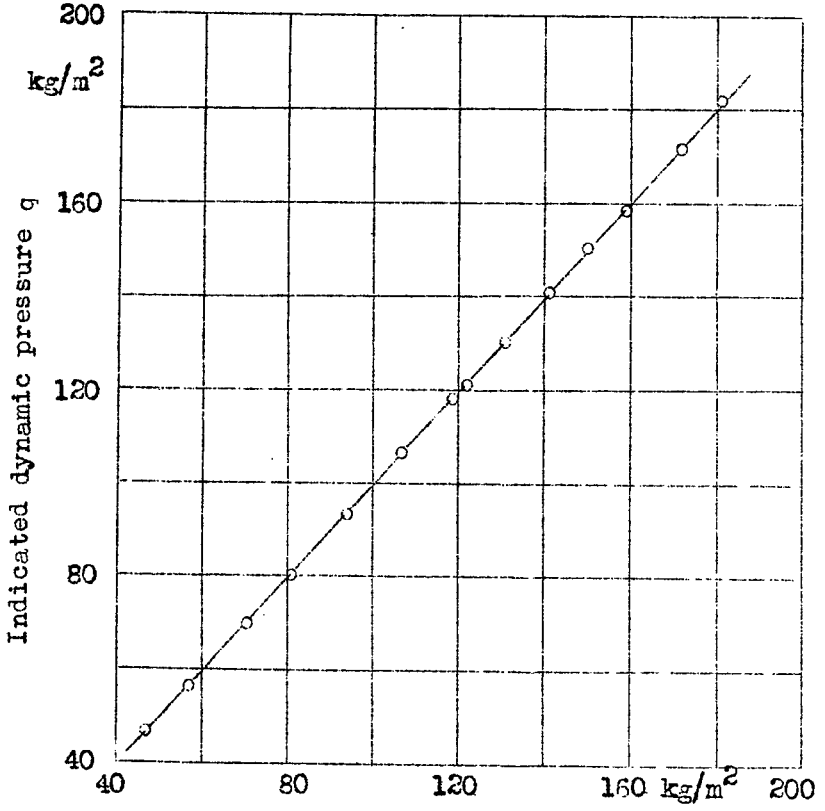

Figure 6.- Calibration of the pitot head mounted at the undisturbed position between the biplane wings.

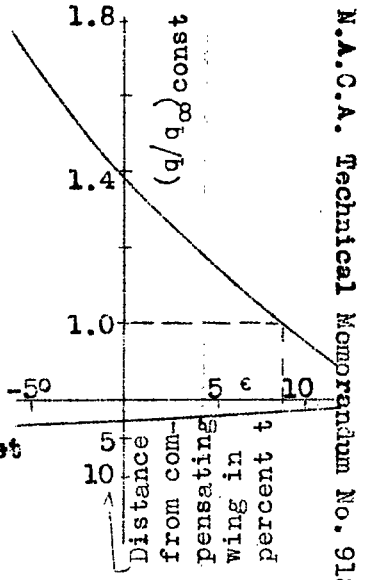

Figure 10.- $(q/q_\infty)_{const}$ and corresponding distance of static pressure orifice from the lower side of the compensating wing as functions of the compensating wing setting ε.

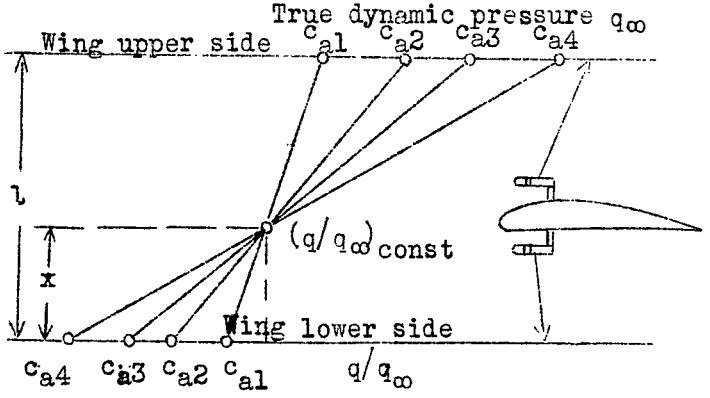

Figure 13.- Sketch showing the determination of the value $(q/q_\infty)_{const}$ over the entire flight range and the location of the static pressure orifice.

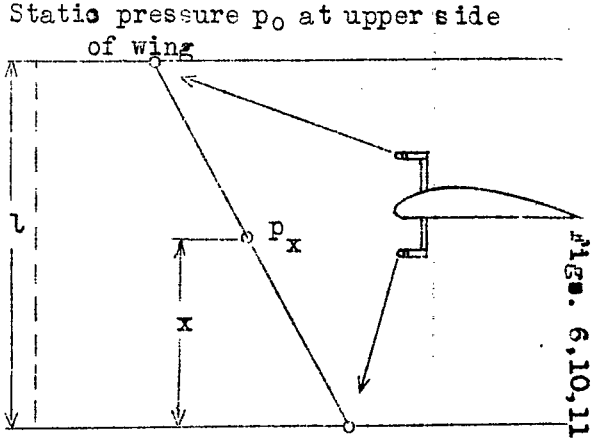

Figure 11.- Explanatory sketch.

Figs. 6,10,11,13

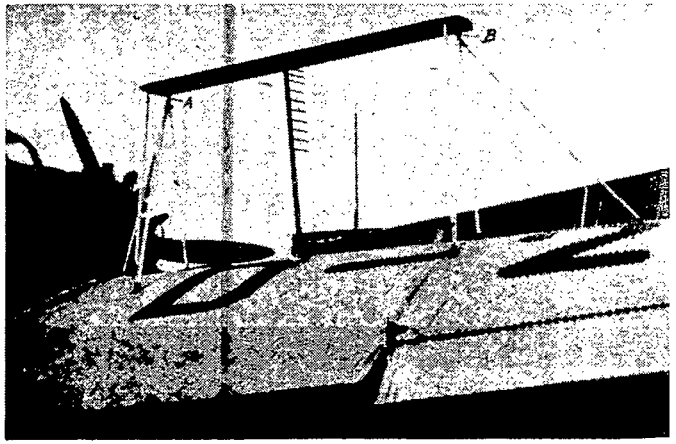

Figure 7.- Compensating wing with pitot heads. The compensating wing is rotatable about the points A and B. By displacement of the rear strut of the N bracing the setting of the compensating wing may be varied. Distance of the compensating wing from upper side of the main wing is 35 percent of the main wing chord at the measuring position. Profile section of compensating wing is NACA M-12, span 2.0 m, chord 0.3 m. Distance of dynamic pressure measuring plane from leading edge of compensating wing is 13.34 percent of compensating wing chord or 1.414 percent main wing chord t. Distance of dynamic pressure measuring plane from main wing leading edge 31.8 percent of main wing chord at measuring position. Compensating wing area/main wing area = 1/76.7.

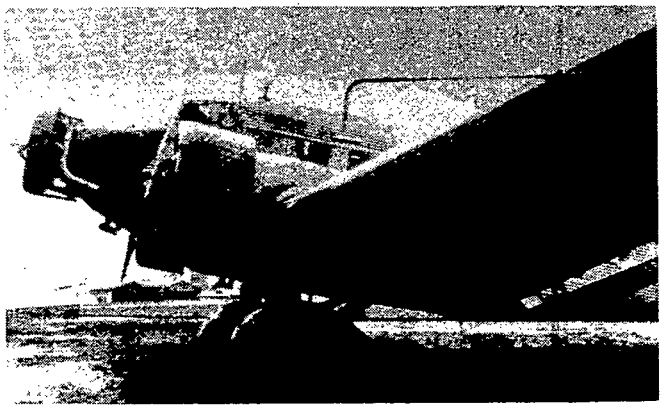

Figure 16.- Pressure head arrangement thus far used on the Junkers Ju 52.

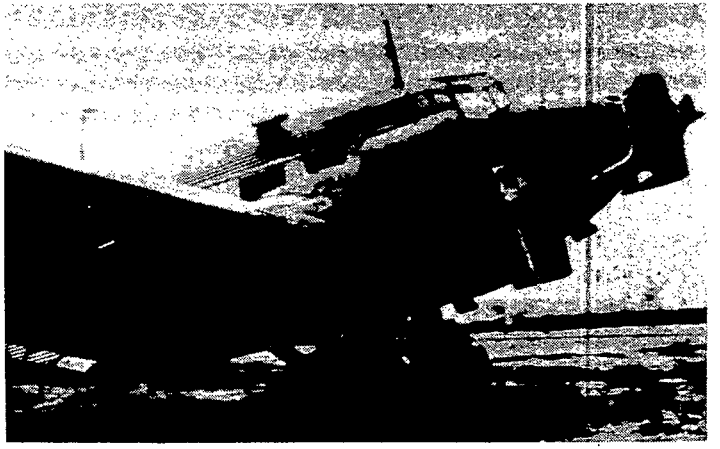

Figure 21.- Final arrangement of double-head installation.

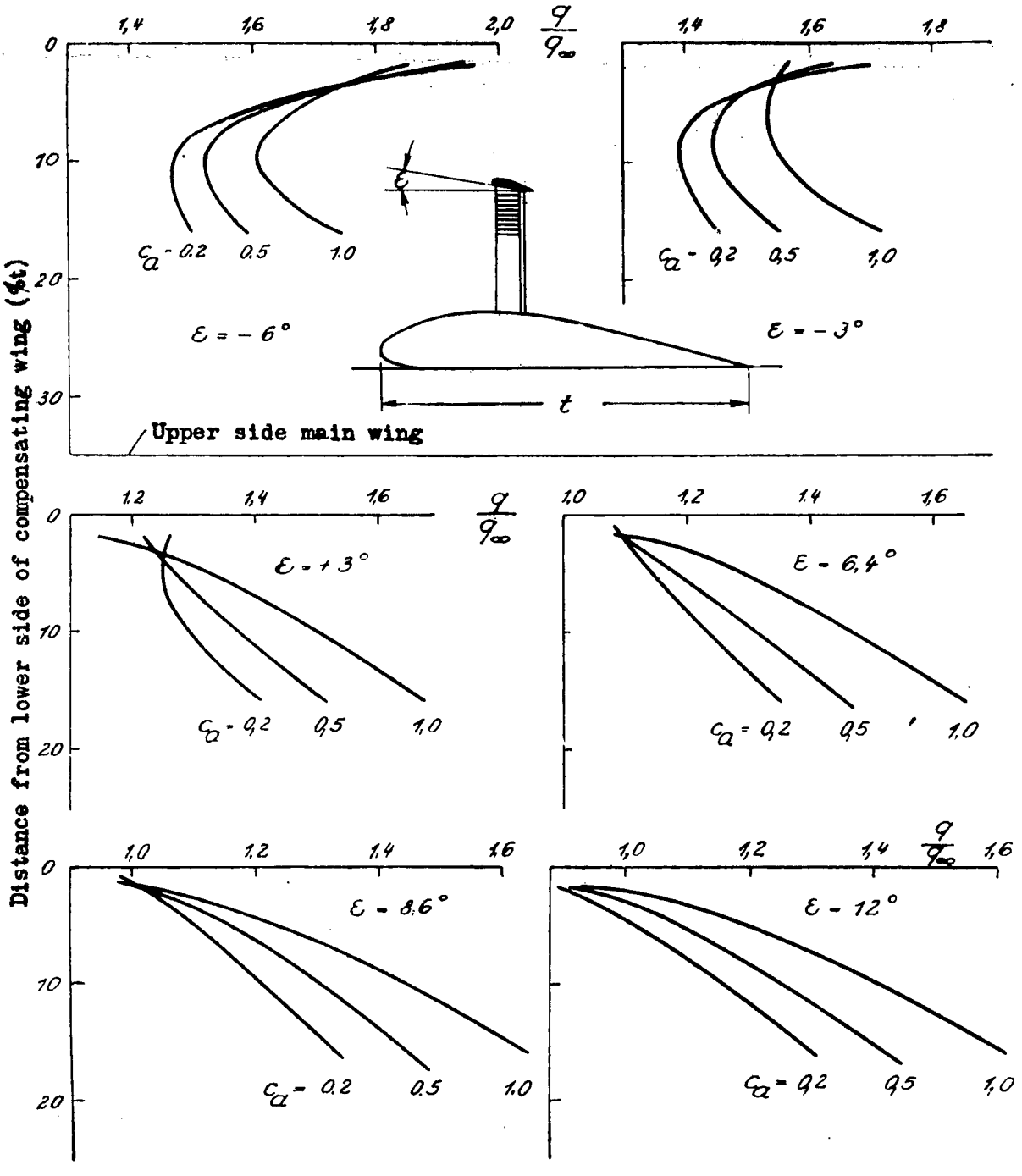

Figure 9.- Dynamic pressure variation between the compensating and main wings for equal settings ε of the compensating wing and various lift coefficients c_a of the airplane.

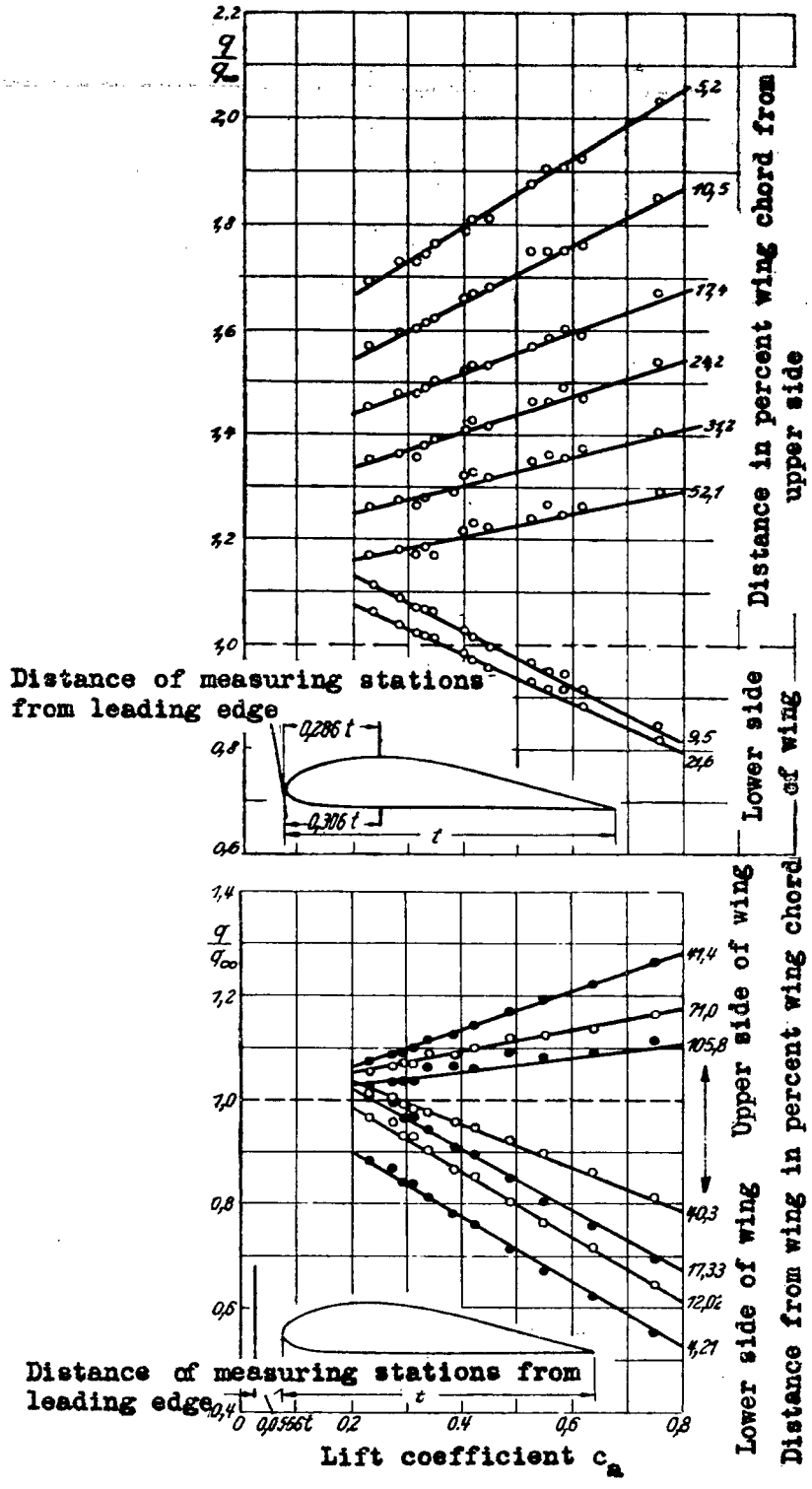

Figure 12.- q/q_∞ as a function of the lift coefficient c_a for various distances from the wing.

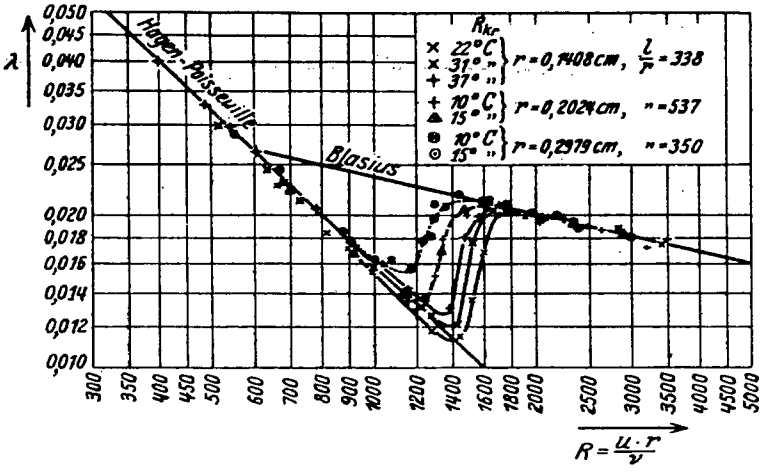

Figure 14.- Drag coefficient as a function of the Reynolds number.

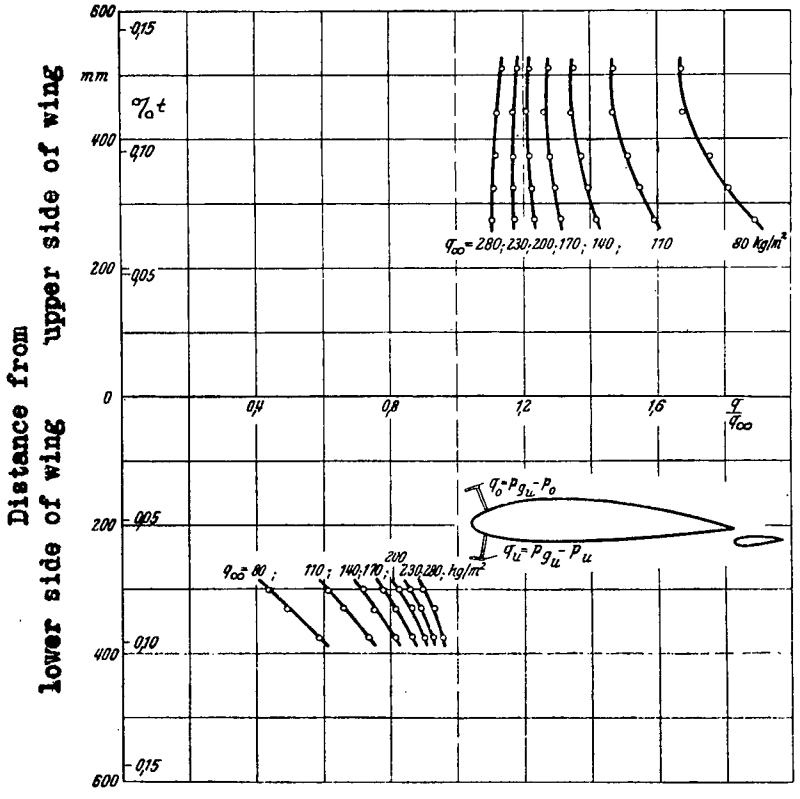

Figure 17.- Dynamic pressure variation in the neighborhood of the wing leading edge.

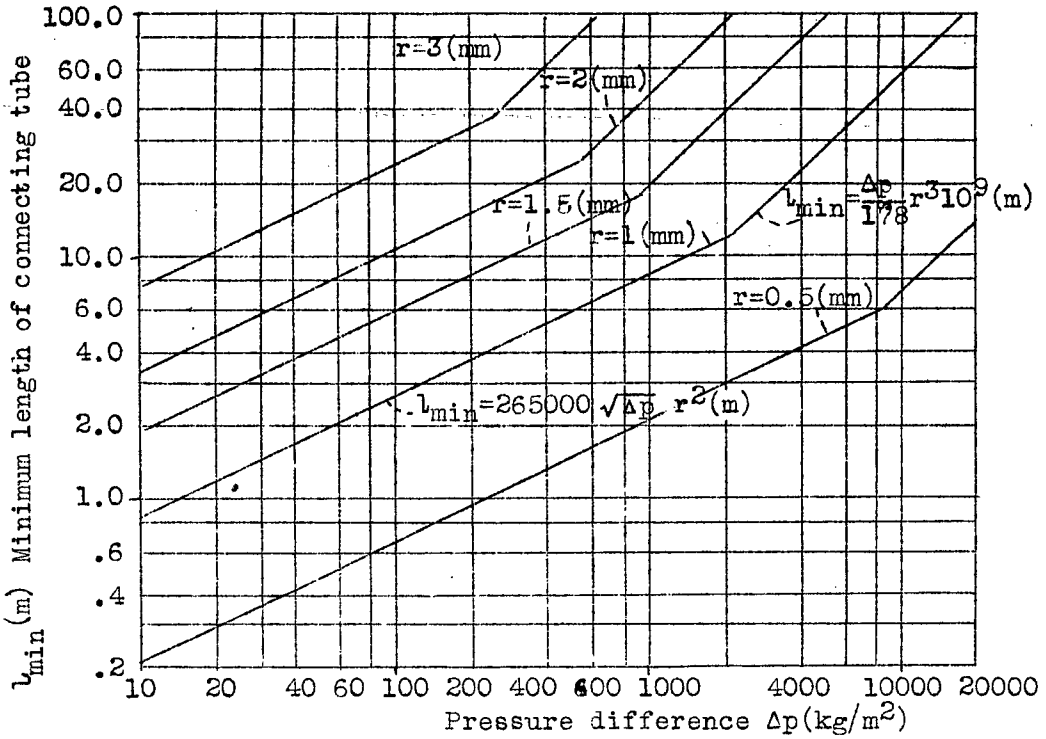

Figure 15.- Determination of the minimum length l_{min} of the connecting tube from the inside diameter r and the static pressure difference Δp.

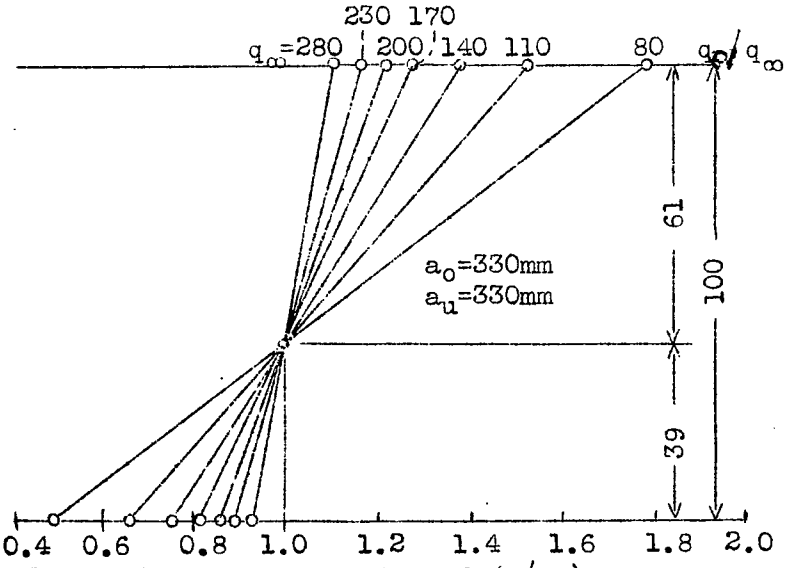

Figure 18.- Determination of $(q/q_\infty)_{const}$ and the corresponding orifice location of the static pressure at the connecting tube. (Distance of static tube from wing upper side a_o=330 mm. Distance of pitot tube from wing lower side a_u=330 mm).

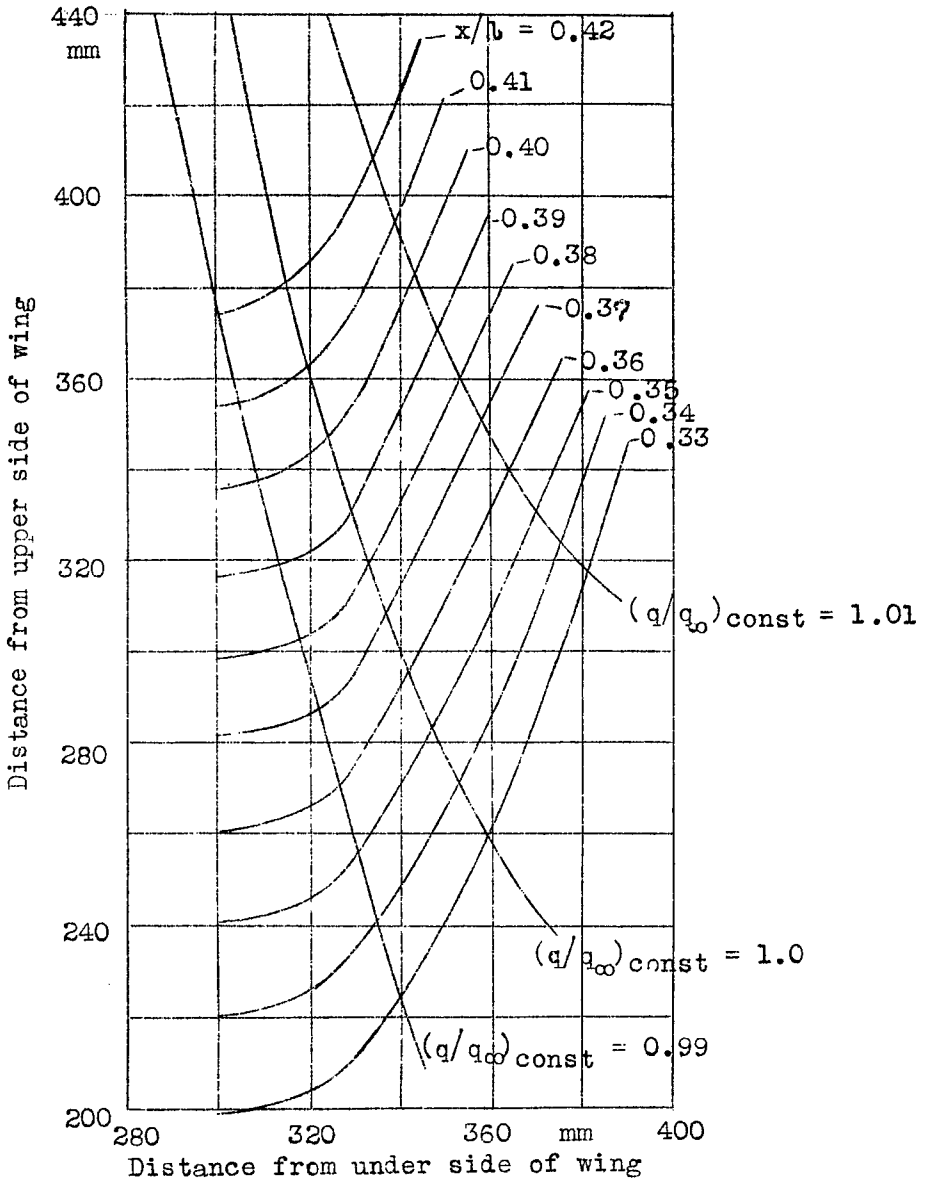

Figure 19.- Location of double-head apparatus for which over the entire flight range $(q/q_\infty)_{const}$ = 1.0, 0.99 and 1.01 and corresponding ratio x/l.

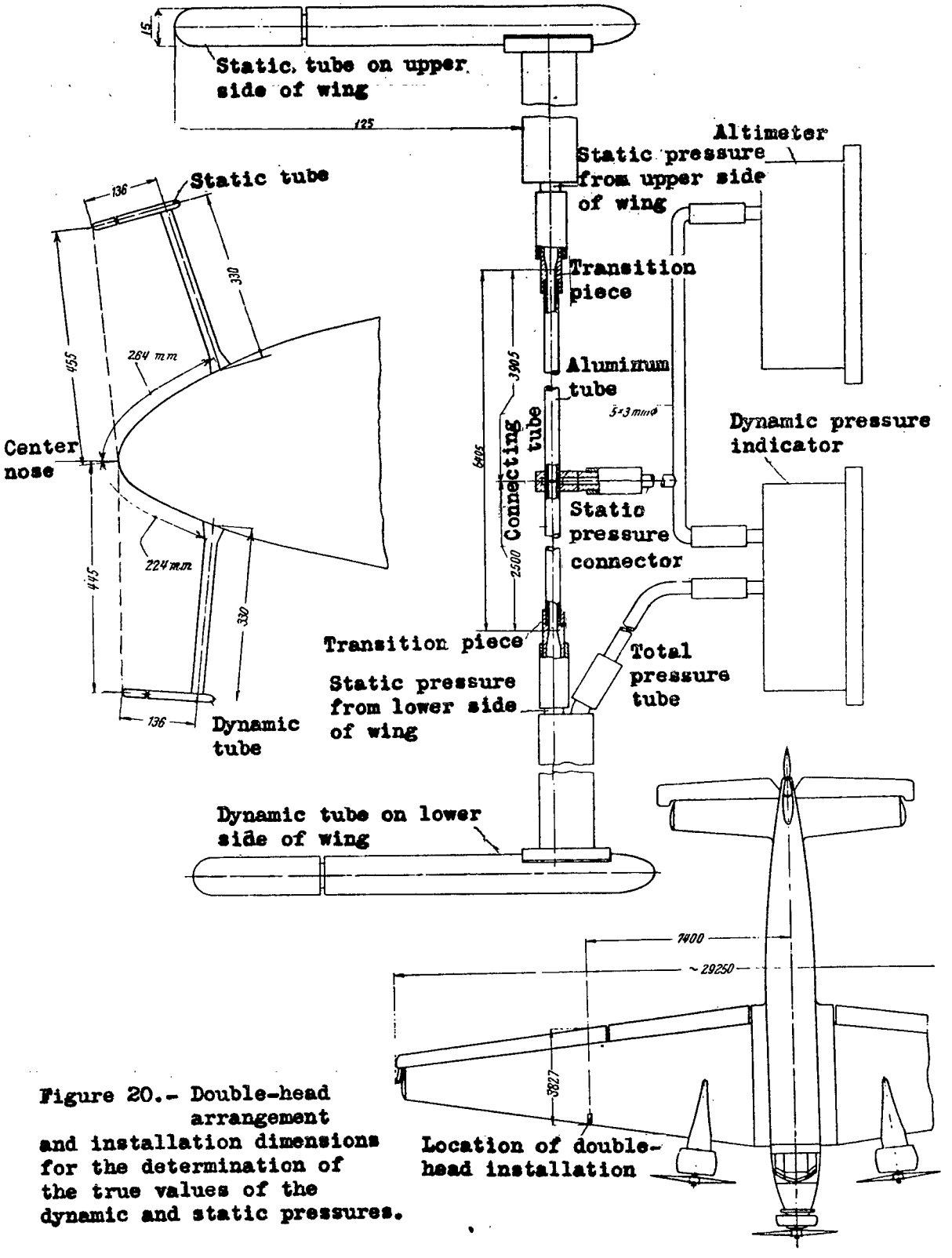

Figure 20.- Double-head arrangement and installation dimensions for the determination of the true values of the dynamic and static pressures.

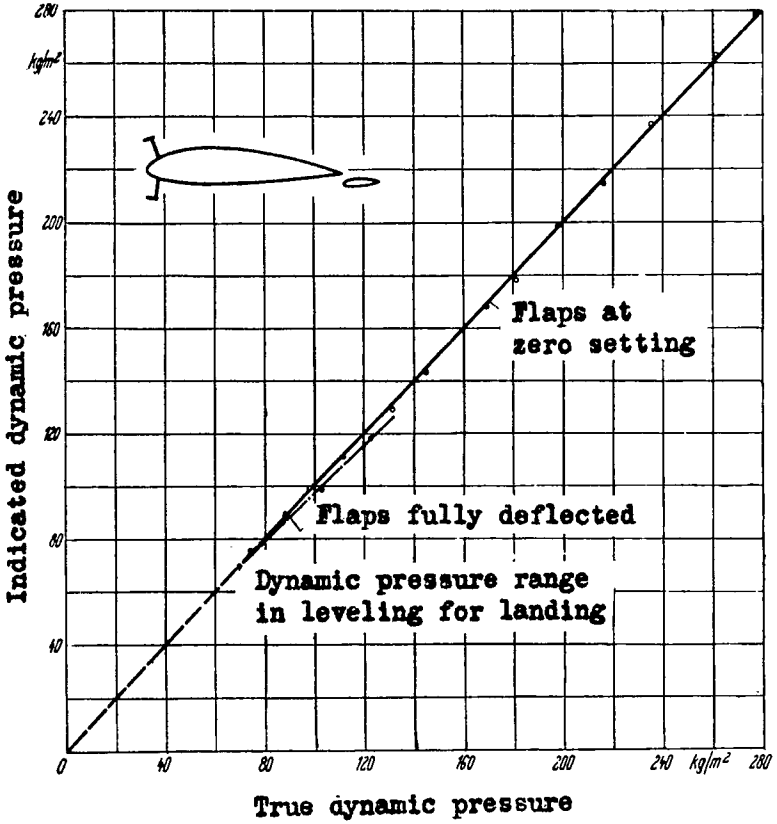

Figure 22.- Check calibration of the final dynamic pressure installation.

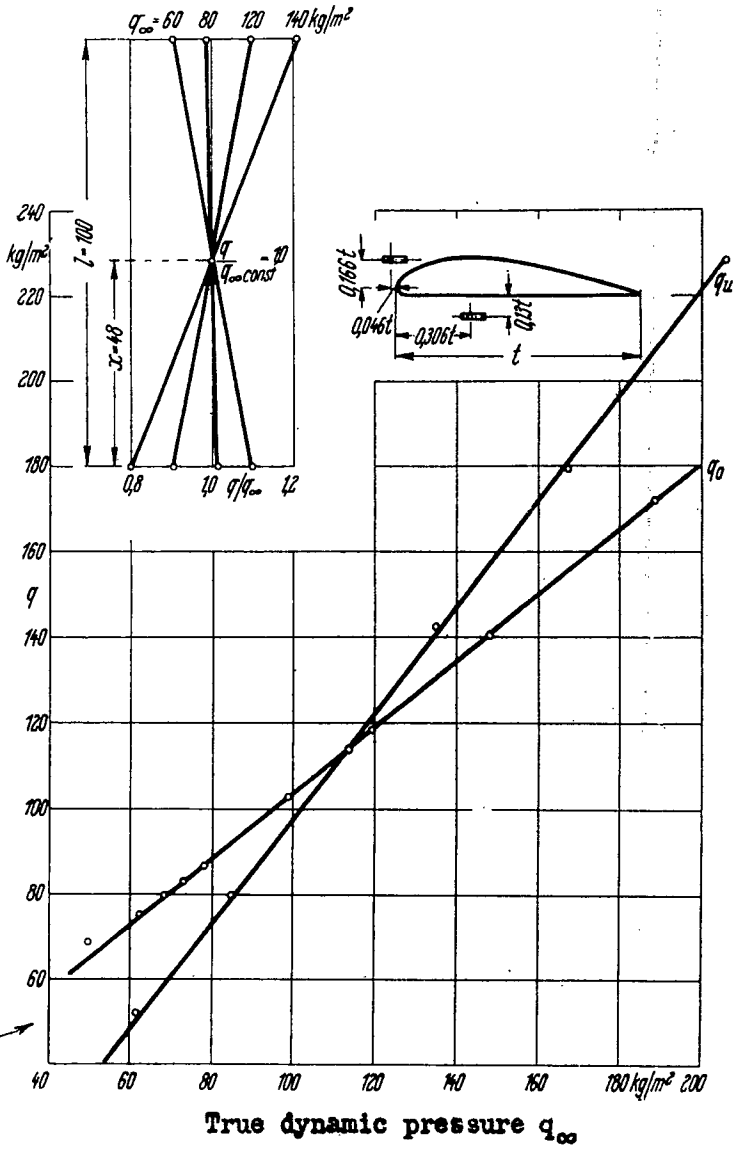

Figure 23.- Example for the direct measurement of the true dynamic pressure for various distances of the static tubes from the wing leading edge. The example shows that the value $(q/q_{\infty\ const}) = 1$ can also be attained if the static tube of the under side of the wing lies further aft than that of the upper side.